September 2017

Title: Changes in metal speciation and mobility during electrokinetic treatment of industrial wastes: implications for remediation and resource recovery

Authors: Claudia Peppicelli[1], Peter Cleall[1], Devin Sapsford[1], Michael Harbottle[1]

Affiliations:

[1] Cardiff School of Engineering, Cardiff University, Cardiff, CF24 3AA, Wales, UK

Corresponding Author:
Michael Harbottle
Cardiff School of Engineering
Cardiff University
Queen's Buildings
The Parade
Cardiff, CF24 3AA
Wales, UK
E-mail: harbottlem@cardiff.ac.uk
Telephone: +44 2920 875759

Abstract

Industrial waste deposits contain substantial quantities of valuable metals and other resources, although often in a recalcitrant form that hinders their recovery. This paper reports an experimental programme on the application of electrokinetic (EK) processing to two different waste materials (a mine tailings deposit and a metallurgical furnace dust), with the aim of exploring the effect of EK on metal speciation and extractability, with a focus on Pb and Zn due to their prevalence in these materials. The speciation of metals within the waste was determined based on a selective sequential extraction (SSE) procedure which was applied to the materials before, during and after the application of the EK treatment. The results demonstrate the generation of an acidic front in the mine tailings, which enhanced the transport of ions associated with the more labile fractions, a behaviour typical of materials characterized by a lower buffering capacity. The application of the EK in the furnace dust showed much less effect due to a very high starting pH (10) with the higher buffering capacity posing an obstacle to transport. It is shown that EK has altered the geochemical speciation of the metals in both materials, typically redistributing them from less available SSE fractions to the more labile fractions. Zn was redistributed with the SSE fractions and mobilised to a greater extent than Pb in both samples. The changes in pH and redox potential arising as a result of the application of an electric field are likely to be the main causes of the changes in speciation of both Zn and Pb. The considerable changes in metal fractionation, including removal from more recalcitrant fractions, suggest that EK may facilitate metal recovery processes. This, combined with its applicability to fine grained materials and heterogeneous environments, demonstrates that the technique may be particularly suited to both remediation of, and in-situ resource recovery from, such materials.

1. Introduction

The application of an electric field to remediate contaminated land, known as electrokinetics, has been used since the early 1990's in countries such as the United States [1] and the Netherlands [2], for the treatment of low-permeability soils containing inorganic (e.g. heavy metals) or organic (e.g. light hydrocarbons) contaminants.

A low voltage is applied between two electrodes set in the ground inducing an electric field in the soil. The main mechanism that governs the subsequent geochemical changes in the pore fluid is considered to be the electrolysis of water, with production of H^+ at the anode chamber and OH^- at the cathode. The acidic environment established at the anode enhances dissolution and/or desorption of metals from the solid phase, which then migrate toward the cathode by electromigration and/or electroosmosis. Ions in solution move by electromigration towards the oppositely charged electrode, whilst electroosmotic transport occurs due to the movement of pore water under the influence of the electric field principally from anode to cathode [3]. As moisture flow occurs due to movement of hydrated ions subjected to an electric field the direction of flow is governed by the net charge on the surface of the solid particles, generally negative, and therefore by the zeta potential (electrical potential at the solid-liquid interface). For a large range of pH, the zeta potential has a negative value, but below the point of zero charge (PZC) it can become positive and therefore lead to a reversing of the direction of osmotic flow. The variation in pH has been identified as one of the key factors controlling the mobility of metals during electrokinetic processes [4, 5] leading to a dynamic geochemistry made up of sorption/desorption, precipitation/dissolution and oxidation/reduction reactions [6].

Waste repositories are not only a potential source of contamination, but also represent a potentially valuable resource. The exploration of technologies able to combine the two aspects, risk reduction and waste valorisation, is central in the contemporary context of circular waste management. Indeed, such is the scarcity of certain materials, waste repositories can be considered as low-grade ores. Crane et al. [7] identified that there are considerable resources available within many industrial waste repositories, however, developing technically feasible and environmentally/socially acceptable approaches for their extraction is a multifaceted problem that requires the application of a low-cost and low-intensity technology. EK belongs to a group of in-situ leaching technologies able to reduce the typical costs of ex-situ processing, avoiding extraction and transport and at the same time applying a process able to generate and control the flow in wastes [8]. In particular, EK operates well in the presence of fine grained materials, as the electric current is not affected negatively by the wastes' particle size, which helps to overcome heterogeneities in hydraulic flow characteristic of other in-situ methods.

Recent studies have explored the application of electrokinetic techniques to industrial wastes such as fly ashes, sludges and mine tailings with the main aim being to stabilise and control the leachability of contaminants from the waste. On application of enhanced EK to anaerobic

digestate Zn and Cu were extracted with removal efficiencies demonstrated to be dependent on the initial geochemical metal speciation [9]. In the case of sewage sludges combining EK with bioleaching allowed the dissociation of metals from the organic fraction for a successful subsequent electromigration [10]. In Pederson et al, the difference in EK removal of metals from MSW incineration fly ashes and wood combustion fly ashes relies on the different degree of metal complexation in the two materials [11]. The treatment of mine tailings highlighted the importance of the use of desorbing agents as acids and complexing agents to enhance the efficiency of EK [12] demonstrating the basic ability of EK to remove exchangeable ions in a similar manner to EK in soil remediation. However, much of the metal resource is often in recalcitrant form, and the ability of EK to affect this bulk resource is still poorly understood. Determination of the speciation of metals by sequential extraction analysis [13] is highly informative in terms of their mobility and extractability. Such studies conducted on the speciation of the metals in mine tailings and fly ashes have shown that metals of interest (e.g. Cd, Cu, Pb, Zn, Cr) are mainly concentrated in the least labile fractions, and are especially present in the sulphide and residual fractions [14]. The study conducted by Kim at al. [14] on tailing soils, characterized by lower concentrations of metals, used a similar approach, but limiting the investigation to the removal of contaminants, it did not show any significant effects on the more strongly bound metals by the EK treatment. Here, via an in-depth study of the mineralogical composition and changes in speciation, the potential of EK is reassessed to shift its focus towards the resource recovery application.

The aim of this study is to explore the impact of an electric field on transport, availability and extractability of metal resources from industrial wastes. In particular, this study seeks to develop understanding of the changes to the distribution of valuable metals between the easily accessible (exchangeable or adsorbed) and the less accessible (oxidisable, reducible and residual) fractions. Whilst it is expected that the former may be transported and extracted more easily, the effect on the latter, where much of the resource may be located, is unknown. This paper reports results of an experimental programme on the application of electrokinetic processing to two different waste materials: from mine tailings deposits and a metallurgical processing waste stream. The speciation of lead and zinc in particular are studied as they are present at elevated concentrations. The association of Pb and Zn with different extractable fractions were determined based on a modified Tessier [15] selective sequential extraction (SSE) scheme.

2. Materials and Methods

2.1. Waste materials

Two materials were investigated: a mine tailing and a metallurgical waste. The mine tailing (MT) comes from Frongoch, a former lead and zinc mine in the Ystwyth catchment of mid-Wales, UK. The metallurgical waste is an electric arc furnace dust (EAFD), a product of the processing of steel scrap metal in an electric arc furnace. The dust was collected from the dust

hoppers of the air pollution control system of the EAF plant. MT and EAFD materials were collected and stored in sealed containers at 4 °C. Prior to use, both materials were well-mixed to minimise variability between specimens and experiments.

2.2. Analytical methods

2.2.1. Metals concentration and Selective sequential extraction (SSE) method

Heavy metal concentrations in the waste materials were determined by microwave acid-digestion followed by analysis by ICP-OES. 3 ml of concentrated nitric acid, 3 ml of concentrated hydrochloric acid and 2 ml concentrated hydrofluoric acid was added to approximately 0.100 g (accurately known) of material prior to microwave-assisted digestion (Anton Paar Multiwave 3000). Concentrated boric acid (12 ml) was subsequently added before filtration through a 0.45 μm cellulose acetate membrane filter and dilution to 50 ml with deionised water and analysis by ICP-OES (Perkin Elmer Optima 2100 DV ICP-OES). Preliminary experimentation identified the ranges of concentrations expected during ICP-OES analysis. Therefore the ICP-OES was calibrated around those expected values and where necessary liquid samples were diluted to reach these reliable ranges of measurement.

In order to allow comparison between materials, a single SSE scheme has been utilised. The Tessier method [15], modified as described by Forstner [16], was employed (Table 1). This splits the oxyhydroxide target phase extraction into two steps: a milder reduction for manganese oxyhydroxides and amorphous iron oxyhydroxides, followed by a stronger reduction of the well-crystallized iron oxyhydroxides. This method is fully described by Mester and Cremisini [17], and was used by Dold [18] to assess the metal speciation in mine tailings. It resembles the scheme used by Hansen and Pedersen [19] with combustion fly ashes, and in MSW by Esakku and Selvam [20].

The time and conditions of each extraction step are reported in Table 1. Initially, 0.500 g samples were dried in an oven at 105 °C for 2-3 h and weighed. All the extractions were carried out in 50 ml polypropylene centrifuge tubes, and were performed by shaking in a mechanical shaker to ensure that solids were continually kept in suspension during the extraction. The extract was separated from the solid residue by centrifugation at 1969 rcf and filtration through a 0.45 μm filter paper. The residue was washed by adding 10 ml of deionized water, shaking for 15 min and centrifuging. The wash supernatant was discarded, taking care not to discharge any of the solid residues which underwent the following step. When an adjustment of pH was required by the procedure, this was done by adding nitric acid (2 M).

Table 1: SSE scheme. r.t. = room temperature. CE= cation exchange, OAc=acetate

Step	Fraction	Normal target phases	Chemical Used	Duration, temperature
1	Exchangeable, water soluble	Soluble species, CE sites.	10 ml, 1 mol l^{-1} ammonium acetate, at pH=7	2 h, r.t.
2	Carbonatic phase	Metals precipitated as Carbonates	10 ml, 1 mol l^{-1} sodium acetate, at pH=5	5 h, r.t.
3	Easily reducible	Manganese oxyhydroxides and amorphous iron oxyhydroxides	50 ml, 0.1 mol l^{-1} hydroxylammonium chloride at pH 2	12 h, r.t.
4	Moderately reducible	Crystallized Iron oxyhydroxides	50 ml, 0.2 mol l^{-1} ammonium oxalate, at pH=2	24 h, r.t.
5	Oxidisable	Organic matter and sulphide	10 ml, 30% H_2O_2; once first reaction is over, 25 ml 1.0 mol l^{-1} ammonium acetate, at pH 2	1 h manual shake + 3 h at 85 °C in sand-bath for the extraction with H_2O_2, 16 h at r.t with NH_4OAc
6	Residual		6 ml HNO_3 + 2 ml HF + 2 ml H_2O_2 digestion	

Samples obtained with this methodology were stored at 4 °C and subsequently submitted for ICP-OES analysis.

2.2.2. Material characterization

For the material characterization MT and EAFD were dried and mixed (using a mixing pad), using the fraction sieved past 2 mm and sub-samples were created by riffling down to obtain an appropriate mass for the analysis technique. The mineralogical composition was investigated by x-ray diffraction analysis (Philips PW1710 Automated Powder Diffractometer using Cu Kα radiation at 35 kV and 40 mA, between 2 and 70 °2 Θ at a scan speed of 0.04 °2 Θ/s) and the phases were identified using Philips PC-Identify software. The microtexture and the imaging of sub-micron features were also studied by SEM analyses with a Zeiss Sigma HD Field Emission Gun Analytical SEM on samples before and after the treatment.

The particle size distribution for subsamples of dried material was determined using a MasterSizer 3000 (Malvern). Paste pH was measured in triplicate in deionised water in a liquid-to-solid ratio (L/S) of 2.5 after shaking and standing for 8 h [21]. Specific gravity was determined using the pycnometer method for fine grained soil [22] with a triplicate measurement.

2.2.3. Electrochemical properties: Zeta Potential investigation and buffering capacities

The variation in zeta potential with pH was determined based on the methods of Vane et al. [23] and Kaya et al. [24, 25], in order to assess the presence of (or lack thereof) a PZC and therefore the direction of the electroosmotic flow. The fine fraction of the dried material was obtained by dry sieving past 63 µm for 15 minutes [25]. A sub-sample of fines was suspended in deionized water (0.2 g in 200 ml) in a volumetric flask and kept in suspension using a magnetic stirring bar [25]. The pH of the suspension was adjusted by dropwise addition of hydrochloric acid (1/0.1/0.01 M according to the accuracy of the adjustment) or sodium hydroxide (1/0.1/0.01 M) solutions. After shaking overnight (20-24 h), the pH was readjusted to the desired level, if necessary, before zeta potential determination (Zetasizer Nano, Malvern Instruments).

The acid neutralization capacity (ANC) of the wastes was determined using a titration procedure [26] which manually adjusted the pH in samples with a L/S ratio of 10 to cover a range of investigation from pH 1 to 12. It was possible to assess the amount of acid (moles of H^+) or base (moles of OH^-) needed to reach a given final pH in a waste. This information was used to evaluate the strength of the acid front needed to influence the leaching behaviour of the materials base on their buffering capacity.

2.3. Electrokinetic experiments

The electrokinetic experiments were carried out in acrylic containers (Figure 1) for a duration of 28 days. Duplicate tests were carried out on each material, MT1-MT2, and EAFD1-EAFD2.

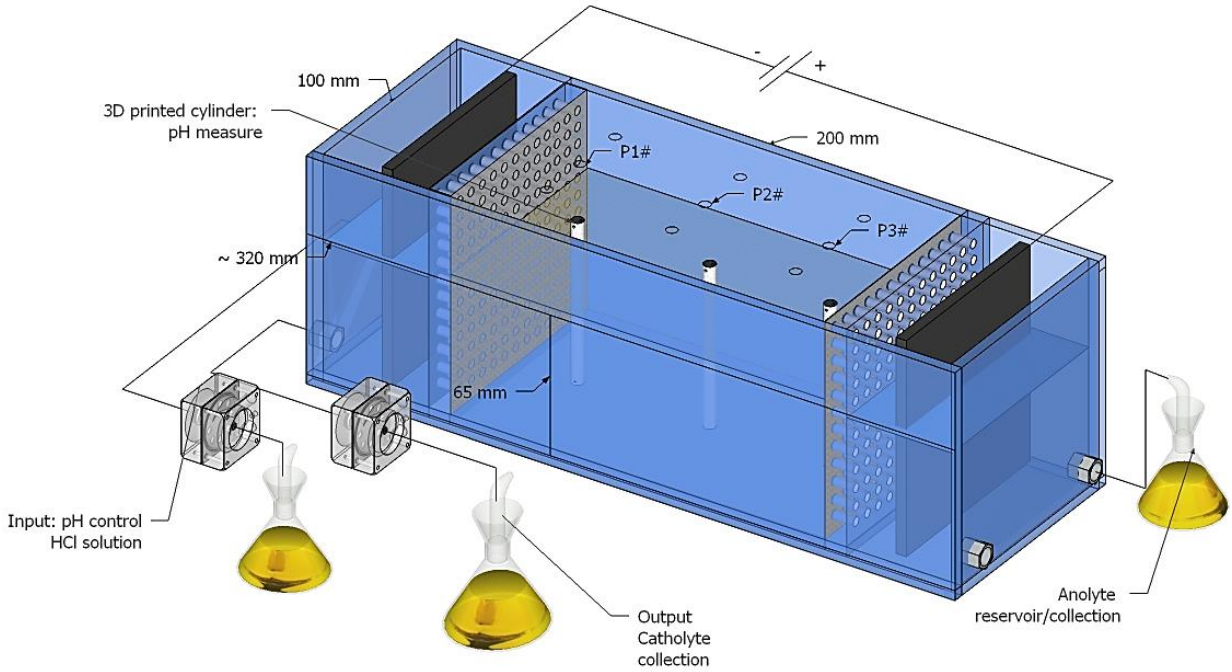

Figure 1. Schematic diagram of electrokinetic cell.

The central, 200 mm long, chamber holds the waste material, separated from electrode chambers at either end by a 10 mm thick perforated acrylic plate lined with coarse-grained filter paper. Wastes were placed, compacted and allowed to settle under a constant atmospheric pressure for 1 week, for a total depth of 65 mm. The total dry weight was approximately 1.9 kg of MT and 1.7 kg of EAFD. The difference in weight given in the same volume is due to a larger porosity of the EAFD (0.7) compared to the MT (0.6). A difference in hydraulic conductivity does not affect the EK test since voltage rather than hydraulic gradients drive the main processes. Following placement of the waste, the electrode chambers were filled with deionized water as an electrolyte and left under a constant head for one week until no further head loss was observed to ensure the material was as close as possible to full saturation. The starting moisture content was of 38% for MT and 70% for EAFD. Compressed graphite plate electrodes, 100 mm high 90 mm wide and 10 mm thick, were installed in the electrode chambers.

In order to avoid elevated pH in the cathode chamber, which would (i) decrease the ability of the system to extract the metals, (ii) increase the voltage gradient in the waste near the cathode and (iii) lower the current, a pH control system was implemented. A peristaltic pump was used to dose HCl solution (0.1 M) into the cathode chamber to maintain the pH in a range of 4-6 and at the same time flush out the solution that was extracted from that end for collection. The anode compartment was connected to a Mariotte bottle to provide deionized water and maintain a constant level of electrolyte solution to a set overflow. The entire apparatus was covered with removable film to control and reduce evaporation as much as possible.

Power was supplied by a bench-top power supply (max 30 V) and current was monitored by a digital ammeter. The aim was to maintain where possible a constant current of the order of 20 mA (0.4 mA/cm^2). When this condition could not be sustained the system was run at constant voltage, the electric gradient applied was 0.5 V/cm. A current density of the order of 0.2-0.9 mA/cm^2 with a constant voltage of 0.5 V/cm is comparable with those in literature [27].

During testing, the pH was measured in the electrode chambers. Three points of pH measurement across the specimen were added, as can be seen in Figure 3, inserting 3 small 3D-printed cylinders (polylactic acid, 4 mm internal diameter, 80 mm height) across the full depth of the specimen to collect the pore water. The walls of the cylinders contained numerous small holes of 1 mm diameter across the entire surface to allow pore water to flow through. To avoid entrance of solids the external surfaces were covered with a nylon membrane (45 µm pore size). A micro pH electrode (3 mm diameter, InLab Micro, Mettler Toledo) was used to record pH in these cylinders and the electrode chambers at intervals.

A core borer of 6 mm internal diameter, pushed down through the whole depth of the specimen, was used to take three samples from each specimen after 0 (t0), 14 (t1) and 28 (t2) days, at the following locations: Position 1 - close to the cathode (3 cm from cathode wall),

Position (central), and Position 3 - close to the anode (3 cm from anode wall); as indicated on Figure 1 with the labels P## (the first number refers to position (e.g. P1# is close to the cathode), whilst the second refers to the time (e.g. P#2 is taken at sample time 2 i.e. after 14 days)). Metal concentrations in electrolyte solutions were measured once a week from the solution overflowed from the cathode chamber and from samples collected directly at the anode chamber. The volume in the overflow bottle and chambers was recorded when they were emptied to calculate the concentration at that time and start with a new time interval. The content was filtered at 0.45 µm and both the solution and the filtered solid residue analysed for total metal content by ICP-OES, the latter after acid digestion.

2.4. Statistical treatment

All the initial characterization analyses of the materials (total metal concentration and SSE at time 0) were carried out in triplicate with the average reported alongside the standard deviation. All other data were obtained from duplicate experiments, and are presented as average values with error bars describing the range.

3. Results and discussion

3.1. Materials characteristics

Characteristics of the experimental materials are presented in Table 2 with clear differences in the composition of the materials. The XRD analysis for MT and EAFD highlights the presence of the metal-bearing phases for Pb and Zn. Although the quantitative XRD analysis does not fully agree with the more accurate ICP analysis of total Pb and Zn (also in Table 2), it is considered a valuable indication of the likely minerals present and their proportions. MT shows an appreciable proportion of sphalerite (ZnS), galena (PbS) and anglesite ($PbSO_4$), while the mineralogical composition of EAFD does not show any explicit Pb-bearing minerals but zinc and iron are present in mineral phases like zincite (ZnO) and the spinel group mineral of magnetite (Fe_2O_4). SEM images of MT (Figure 2a) illustrate an example of a random dispersed sample of MT at t0 with the majority of darker particles (e.g. spectrum 41) that comprise the quartz dominant fraction of the material. The particles of size slightly smaller than 50µm of a bright colour with presence of Pb-bearing mineral phases (spectrum 44) agree with the XRD detection of galena and anglesite. Spectrum 42 characterizes particles of grey colour slightly larger than 50 µm with presence of Zn-bearing mineral phases, confirming the presence of sphalerite.

Table 2. Materials characterization (ranges where given are +/- 1 SD, n=3).

Property	MT	EAFD
Particle size distribution	71% fine sand(>63 μm), 27% silt (>2 μm), 2% clay (<2 μm),	9% fine sand (> 63 μm), 85% silt (>2 μm), 6% clay (<2 μm),
Mineralogical composition (XRD)	Quartz (69%), Sphalerite (7%), Muscovite (12%), Galena (5%), Anglesite (5%)	Zincite (46%), Magnetite (42%), Hydrotalcite (4%), Hibonite (4%), Hydrozincite (2%)
Specific gravity (g/cm^3) (BS 1377-2)[22]	2.911 +/- 0.023	4.555 +/- 0.047
pH (BS 1377 -3)[21]	5.8 +/- 0.7	10.5 +/- 0.2
Total Pb content, raw material (wt% and range)	5.1 +/- 0.1	2.2 +/- 0.5
Total Zn content, raw material (wt% and range)	2.5 +/- 0.3	32.1 +/- 2

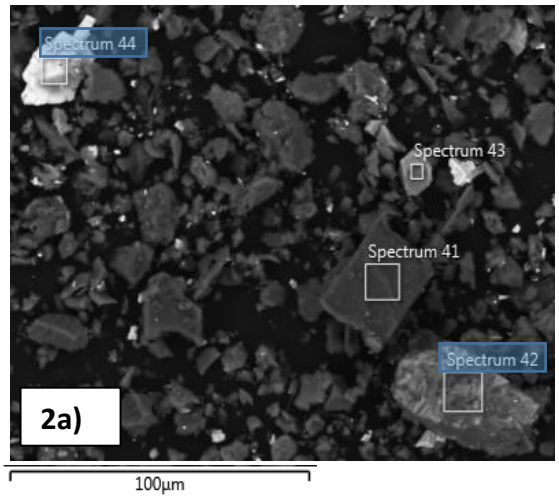

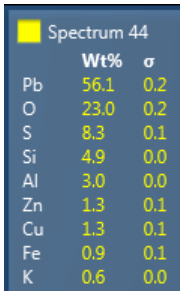

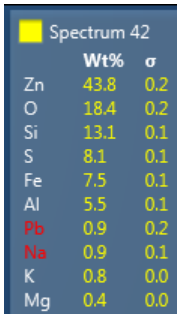

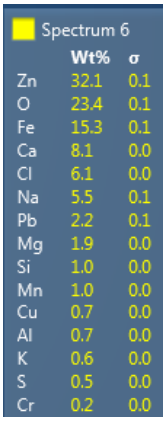

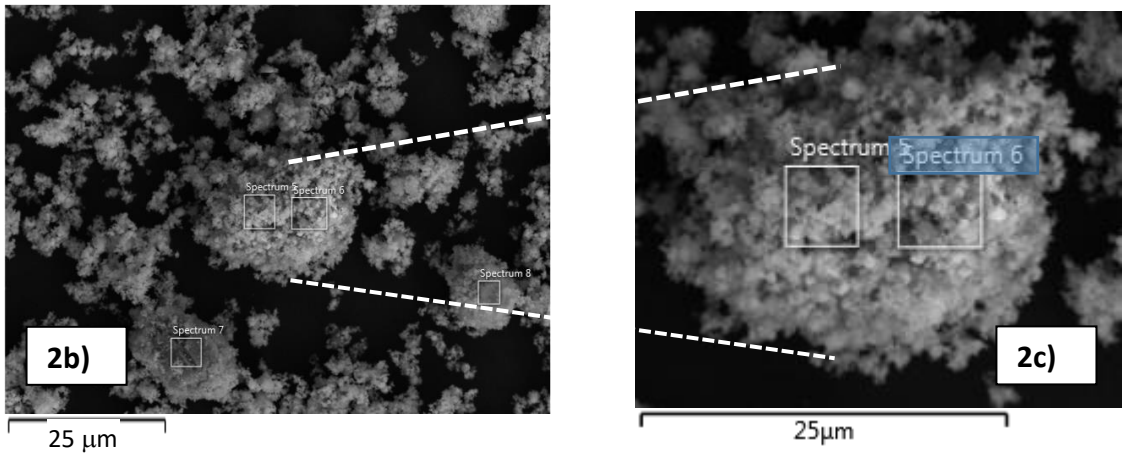

Figure 2. **Back-scattered scanning electron microscopy** images of MT (a) and EAFD (b), individual EAFD particle (c).

The particles shown in Figure 2b are typical of those observed in a random dispersed sample of EAFD at t0 - similar images are found in literature [28-30]. The enlarged image (Figure 2c), shows that these are characterized by an irregular shape and surface. As suggested by Stegemann et al [29] this could be due to agglomeration of the spherical spinel minerals of magnetite and metal oxides. Spectrum 6 demonstrates that these are composed of Fe-Zn oxides in agreement with the magnetite and zincite detected by XRD. SEM-EDX characterisation of EAFD by Machado et al [30] suggested that regions with high presence of Zn and Fe can be identified as spinel franklinite phase ($ZnFe_2O_4$) but that the overlapping of the signals with the magnetite could not unequivocally define the phases. Furthermore Laforest et al [28] working on a similar furnace dust observed that most of these particles were a solid solution of magnetite-zincite. In these studies, elevated concentrations of other metals, like Pb in this case, can be found in association with the main spinel group (magnetite) for the characteristics of partial substitution of the iron with other cations [30].

The initial Pb and Zn contents of the raw materials are presented in Table 3, showing the distribution across the six fractions determined by selective sequential extraction.

Table 3. Concentration distribution of metals in the two materials prior to EK treatment (ranges are +/- 1 SD [n=3], whilst percentages represent the proportion of the total metal recovery in that material).

Target Fraction	**Pb**		**Zn**	
Values in (mg/kg)	**MT**	**EAFD**	**MT**	**EAFD**
Exchangeable **(f1)**	16,218 ± 532.9 (31%)	2,758 ± 259.5 (10.5%)	1,147 ± 79.2 (4.5%)	26,506 ± 1,736 (4.9%)
Precipitated as carbonates**(f2)**	13,857 ± 437.7 (27%)	12,751 ± 728.0 (48.8%)	255 ± 9.4 (1.0%)	98,024 ± 4,365 (18.3%)
Mn-oxides/ Easily Reducible **(f3)**	7,742 ± 382.2 (15%)	1,823 ± 39.6 (7.0%)	580 ± 8.8 (2.3%)	112,271 ± 6,130 (20.9%)

Fe-Oxides/ Moderately Reducible **(f4)**	352 ± 22.0 (0.5%)	369 ± 11.5 (1.4%)	333 ± 15.4 (1.3%)	3,574 ± 146.2 (0.7%)
Sulphides/ Oxidisable **(f5)**	5,664 ± 683.3 (11%)	4,148 ± 389.0 (15.9%)	22,772 ±4,775 (88.5%)	8,211 ± 7.5 (1.5%)
Residual **(res)**	7,979 ± 1,835 (15%)	4,302 ±1,597 (16.5%)	644 ± 64.0 (2.5%)	288,114 ± 4,441 (53.7%)

Whilst the majority of Pb (>50%) in MT is distributed between the most available fractions (f1 and f2) that have previously been described as representing the electrokinetically-accessible phases [31], there are also appreciable amounts of Pb associated with the recalcitrant fractions. However, it is noteworthy that for MT although sulphides (especially galena) are present, the amount of sulphide-associated/oxidisable lead is relatively small (f5). Zn is predominantly present in f5 (sulphides/oxidisable, 89%) which ties in with the XRD detection of sphalerite (ZnS). These results are also in line with a similar extraction procedure used on a similar tailings collected at the same site by Palumbo et al. [32].

In the EAFD, Pb is mostly bound to what would be typically considered as the EK-accessible fractions (predominately f2, approximately 40%) followed by fractions f5 and residual with equal distribution of the Pb at around 15%, and 10% in f3. This distribution is comparable to that reported by Laforest et al [28] for a similar material. The particular association of Pb with fraction f2 and f3/4, when considered alongside the SEM-EDX and XRD data (Figure 2b, Spectrum 6) suggest that Pb is associated with the (i) spinel mineral of magnetite and (ii) bound to carbonates – note the correlation with Ca detected by the SEM-EDX (average 4.3%). In terms of mobilisation, EK would be expected to have a solubilising effect on f2 in regions of the waste where acidic pH develops. Zn shows an initial distribution of 23% in fractions f1 and f2 combined, and a significant proportion (around 20%) bound to oxides (ZnO and FeMnOx detected by XRD), although the dominant fraction is the residual. Magnetite (detected by XRD) is likely to comprise much of the residual fraction given its refractory nature, and that the residual zinc is associated with this.

3.2. pH changes and electrical performance

The anode chamber pH for both materials displayed a rapid decrease during the first 24 hours to values close to 2 and then progressively and slowly reached values around 1 or below (results not presented). The pH in the cathode chamber (Figure 3a) was more variable. Results of pH profiles at the 3 measuring points across the specimens (P1, P2, P3 - from cathode to anode) during the 4 weeks are presented in Figure 3b and 3c. The migration of H^+ ions (generated by the electrolysis of water at the anode) towards the cathode resulted in a gradual lowering of the waste material pH as shown in Figures 3b (MT) and 3c (EAFD). A gradual decrease of the pH across the specimens, particularly close to the anode, was observed in both materials with the exception of position 1 (near the cathode) in EAFD where pH gradually increased. This was caused by the extremely alkaline pH of EAFD combined with

electrokinetically induced pH increase at the cathode, which the pH control system struggled to control (Figure 3a).

Figure 3d shows the results of the ANC test as a measurement of the buffering capacity and resistance of the two materials to acidification. Given the very different starting pH (highlighted in red in Figure 3d), the materials behave in different ways: MT (in grey colour) shows a lower resistance to acidification and is able to reach values of pH around 2 with the addition 0.33 mol H^+ while the EAFD (in blue colour) had a strong acid neutralization capacity, and for the same amount of acid only reached pH 6. These characteristics are reflected in the profiles of the internal pH during the EK test (Figure 3b-c). The high buffering capacity of EAFD compared to MT, demonstrated in Figure 3d, explains why the pH of the material remained above 10 (Figure 3c). Leaching tests conducted by Stegemann et al. [29] on a similar furnace dust indicated that an appreciable amount of Zn and Pb could be released only if a value of pH 6 is reached which corresponds to the plateau of the ANC.

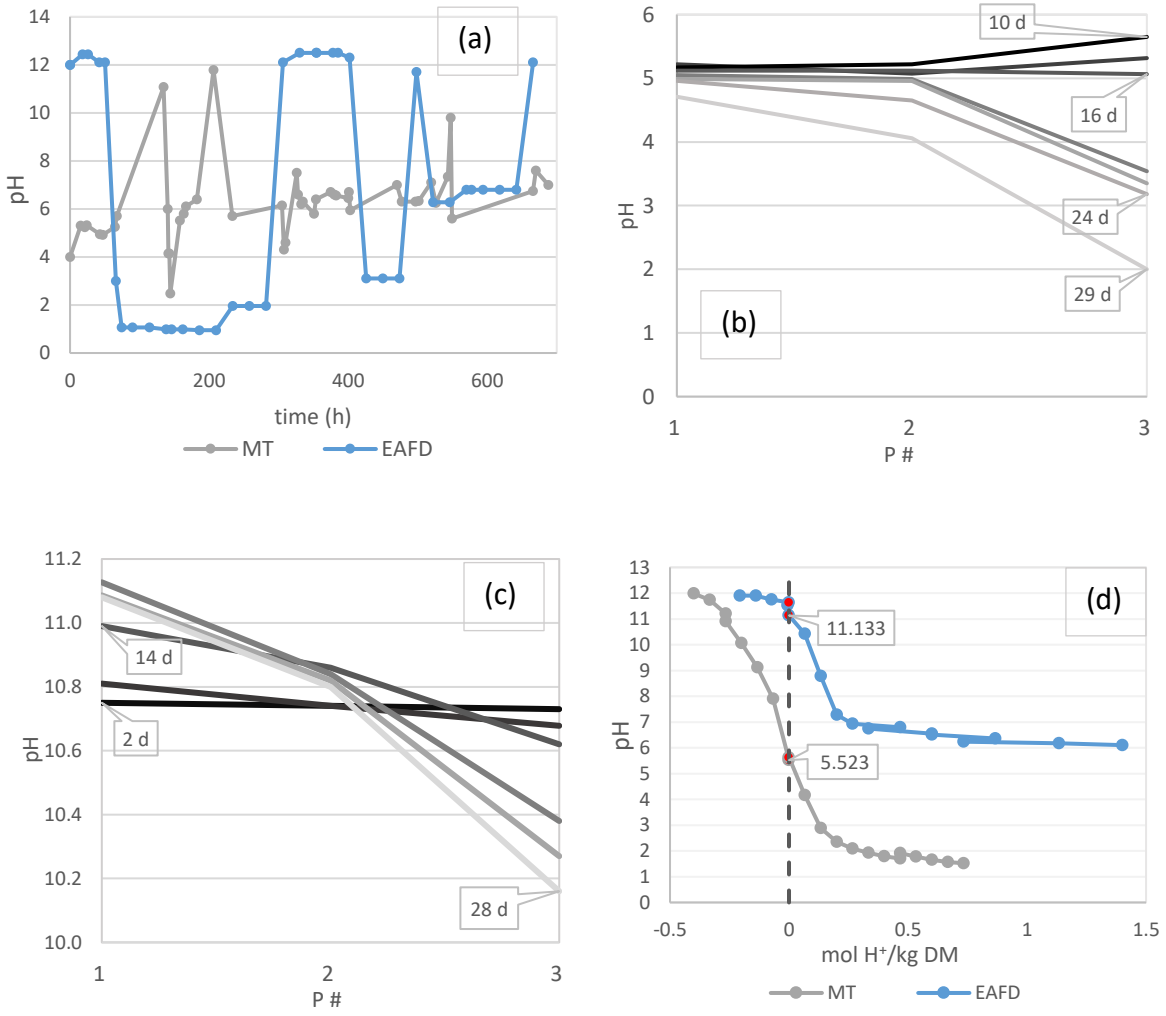

Figure 3. a) pH recorded in cathode chambers. b) pH trend in MT over 4 weeks at position P1, P2, P3 (d – day). c) pH trend in EAFD over 4 weeks at position P1, P2, P3. d) Estimated magnitude of ANC expressed in mol H^+ per kg of dry mass (DM) (Negative values correspond to mol OH^-/kg DM).

Figure 4 shows the overall electrical current applied across the 2 materials during the EK test. MT, where the supplied voltage could not sustain constant current conditions, was treated mostly at a constant voltage of 10 V, with current varying between 10 and 20 mA and an average pH in the cathode chamber of 6 (Figure 3). The variability in current applied over the MT specimens was caused by gradual increases of pH in the cathode chamber leading to precipitation and changes in electrical conductivity (despite constant acid flushing), and subsequent manual adjustments. In addition, a similar effect may have been caused by accumulation of high concentrations of ions in the cathode chamber causing some species to reach saturation - the cathode chamber was emptied and replenished with fresh solution on a weekly basis.

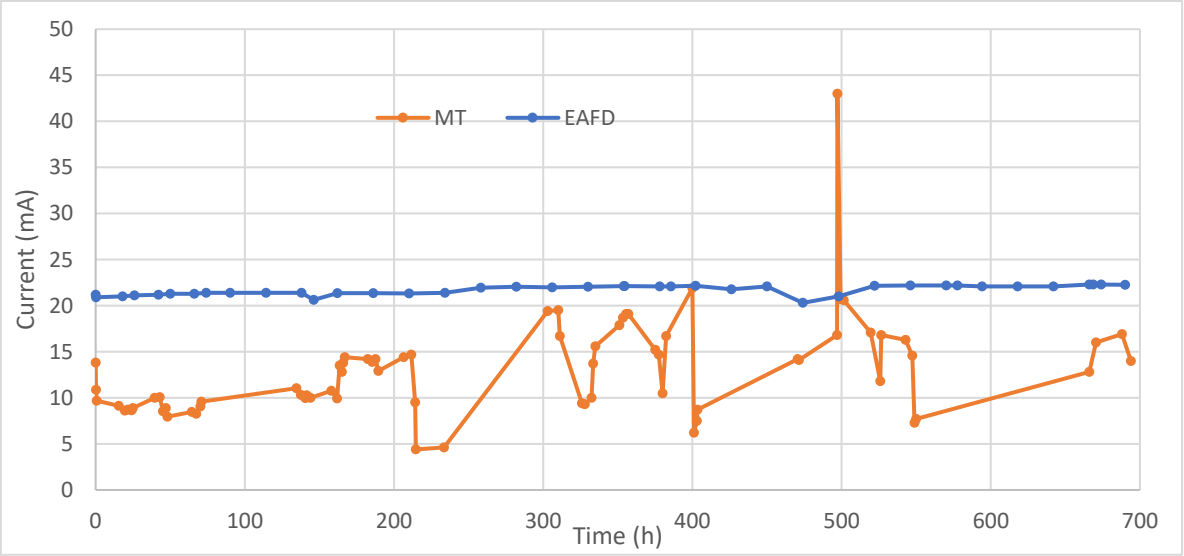

Figure 4. Electrical current applied across the waste specimen during electrokinetic experiments.

EAFD was found to have an electrical conductivity an order of magnitude larger than the mine tailings (14.6 mS/cm compared to 0.2-0.9 mS/cm, measured in a batch leaching test with a liquid to solid ratio of 10 in deionised water). Given the nature of the material and the very high metal content, it is possible that the current flows not only through the pore water, but also through solid particles. It was therefore possible to maintain a relatively constant value of current of 22 mA, with a lower voltage between 2.5 and 3.5 V, for the duration of the experiment.

Despite peaks of energy consumption due to metal precipitation in MT, the voltage was kept at constant levels for EK tests and overall the current did not decrease in time. This could be due to the high concentration of ions in the mobile fractions and the lowering of the pH, the

constant release and migration of metals continues throughout the experiment and helps maintain the current. Similar behaviour was observed by Kim et al. with electrokinetic treatment of tailings soils [33]. This was in contrast to typical remediation experiments [34] when the release of contaminants from the easily exchangeable fractions was exhausted during the test or gradually decreased with time.

Before considering the SSE results it is important to analyse the results of the zeta potential investigation shown in Figure 5. For MT the point of zero charge (PZC) is below pH 2 for this material, indicating that electroosmotic flow would be mainly towards the cathode. The analysis of the zeta potential in EAFD indicates a PZC around pH 6, a pH not reached during EK experiments given the high acid neutralization capacity of the material, suggesting that again electroosmotic flow will be towards the cathode. However, a lower pH may have arisen in the regions immediately adjacent to the anode chamber. The absolute value of zeta potential is lower in EAFD – as the amount of electroosmotic flow [5] is directly proportional to it, the flow may also be expected to be lower in EAFD than in MT.

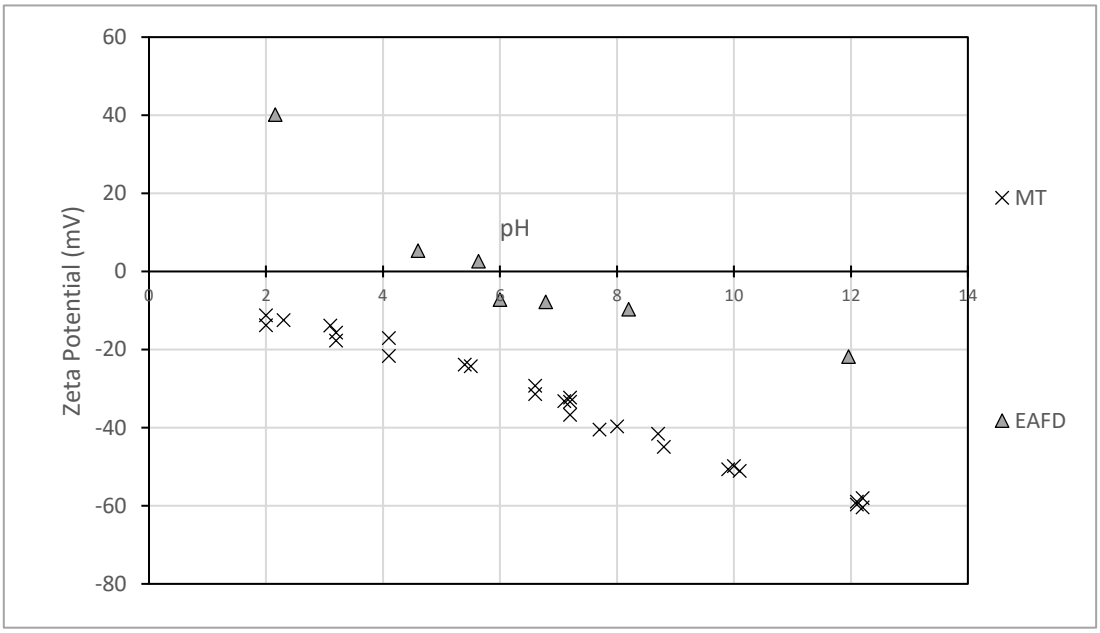

Figure 5. Variation of Zeta potential of MT, EAFD in water as a function of pH.

3.3. Migration and distribution of metals

Analysis of the total metal extraction from the electrode chambers is shown in Figure 6. For MT the majority of Pb and Zn extracted was found in the cathode chamber. The extraction of metals from EAFD was the opposite of that observed in MT, with the majority of extraction observed at the anode. The high pH of the EAFD hindered mobility of both Pb and Zn, but those metals in the more acidified region immediately adjacent to the anode may have been solubilised. Diffusion and the possibility of a reversal of EO flow in this region may contribute to the observed behaviour. A low percentage of extraction was observed with both materials, but with significantly more Zn than Pb extracted.

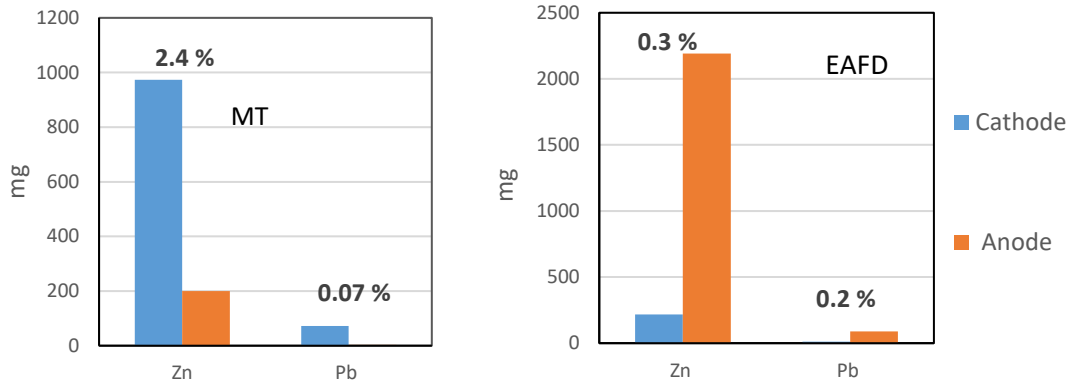

Figure 6. Total metal extracted at electrode chambers at the end of testing (percentage relative to the initial total content).

The variation in concentration of Pb and Zn within the MT and the EAFD is investigated in terms of metal SSE speciation before, during and after the electrokinetic treatment, as shown in Figures 7-12. Figures 7 (MT) and 10 (EAFD) show the metal distributions expressed in mg/kg after 0 (t0), 2 (t1) and 4 weeks (t2) from position p1 (close to the cathode) to p3 (close to the anode). Data are presented as an average of both duplicates. The error bars refer to the variability in the total metal recovery. Recoveries from individual fractions are presented in Figures 8-9 (MT) and 11-12 (EAFD) in a similar manner. Total graphs illustrate overall spatial movement (transport) of the metal, whilst charts of individual fractions illustrate both transport and changes in metal association within these fractions, helping to elucidate the mechanisms of metal redistribution.

From the comprehensive graphs in Figures 7 and 10, it seems that no significant reduction in overall concentration of metals in EAFD has occurred due to the EK treatment. Some of the results show what seems to be an increase in total concentration – it is thought that heterogeneous distribution of metals in the waste may play a role here, as differences in total recovery over time tend to be associated with specimens where there was greater variability initially (t0).

In MT, as figure 8 shows, the concentration of water-soluble Pb (f1) increases with time, especially close to the anode, corresponding to a steady decrease in fraction f2 and f3 directly affected by the changes in pH. Especially at t2 Pb appears to be removed from the residual fraction nearer the anode, with corresponding increases in all other fractions in this location, suggesting that acid generation has significantly altered the distribution of the metal. This may be responsible for leaching the metal from the galena present. The results for Pb suggest a repartitioning of the metal towards the most available fraction.

Zn distributions in MT (Figure 9) are more variable and show possible transport within the material with the pH playing a significant role. The Zn associated with fractions f1, f2, f3 and f4 is most affected by a change in pH, and show increasing concentrations from p3 to p1 that

indicate solubilisation and transport from anode towards the cathode. This is supported by more Zn being extracted into the cathode chamber (Figure 6). Whilst there is an overall reduction in f1 and f4, the fractions f2 and f3 are merely redistributed. F5 also shows a redistribution from anode to cathode, although this is proportionally smaller due to the much larger Zn content in this fraction. This suggests two possible mechanisms affecting ZnS: acid dissolution and oxidation occurring particularly nearer to the anode. This may be partly instigated by the formation of elemental oxygen at this electrode through the electrolysis of water, which has previously been shown to cause an increase of dissolved oxygen transported into particulate media [35]. At the same time the principal oxidant of sulphides in condition of low pH would be Fe(III), with the elemental oxygen that serves to oxidise Fe(II) back to Fe(III) [36].

Overall Figure 9 with its distinctive "staircase" shape SSE profiles, highlights the transport of ions due to the EK typical of materials with a lower buffering capacity.

In EAFD specimens, there is variation in the behaviour between Pb and Zn, and it is difficult to discern any overall substantial trends that allow definitive conclusions (Figures 10-12), possibly because of the higher pH overall and the tendency of metals to be located in less available fractions. Spatial redistribution of either metal in EAFD was much less evident than in MT, which is expected given the higher pH. Although EK has altered the geochemical speciation of the metals from less available fractions to the more mobilisable, it was not enough to enhance extraction within the duration of these experiments.

In Figure 11, the larger changes observed are in the more available forms of Pb (f1, f2 and f4). At time t2 Pb in f1 gradually increases towards the anode, whilst f2 shows an opposite trend. Fraction f4 appears to gradually increase in concentration, especially in p1. This might confirm the effect of the pH in increasing the availability of Pb close to the anode and re-precipitation close to the cathode. For Zn, the distributions (Figure 12) show that at times t1 and t2 there was an overall increase in Zn associated with fractions 1-5, offset by a reduction in the large residual fraction. There appears to be limited spatial redistribution (as indicated in Figure 11), for example f3 having a small decrease close to the anode.

SEM images of EAFD after treatment (Figure 13), when compared with those at time t0 (Figure 2), may help to explain the observed metal behaviour. At point p1 larger particles (250 μm) were observed after treatment, exhibiting a more crystalline nature than the more amorphous and much smaller particles observed at time t0. The SEM spectra at t0 showed average Ca levels of 4.3% which gradually increased to an average of 7.6% in particles close to the cathode at t2. This may be caused by the precipitation of metal salts in this cathode region and corresponding increase in f2 (carbonates) as the presence of these particles, characterized by a similar composition as the one at time t0 (Figure 2b) but with a larger, more crystalline appearance, increases. The particle at location p3 is representative of the majority of particles in this region after EK treatment. Although similar to those at time t0 (Figure 2) they have a more regular shape and better-defined contours. This suggests a

removal of surface-associated minerals such as iron oxides, reducing the Zn associated with such materials which may be attributed to pH and redox effects arising due to EK – for example, a reduction of Zn in f3 is observed particularly in the lower pH region close to the anode.

Overall, the two materials, although very different from each other, show that Zn is mobilized and transported throughout the porous medium during electrokinetic treatment more easily than Pb. Geochemical reactions (dissolution/precipitation, adsorption/desorption) are often pH dependent, but the oxidising environment at the anode could enhance the dissolution of metals from the sulphides phases and residual fractions [37]. The actual extraction of either metal from either material was relatively small, as expected given that the metals are generally integral components of the minerals themselves rather than surface-associated through sorption and other processes, as is usually the case in contaminated soils. However, despite these experiments being only four weeks long it is encouraging to see changes in fractionation, including of the more recalcitrant fractions, which indicate an increase in availability of the target elements. It is apparent that geochemical changes (to pH and redox conditions) have the power to amend availability in these two very different materials, which suggests that further manipulation could enhance extractability. The effect of pH changes on transport and extractability in EAFD in particular are less than those observed in MT due to the much higher initial pH and buffering capacity, but even so substantial change was noted. As expected, a decrease in pH does generally appear to increase both availability and transport; the degree to which this occurs in the most recalcitrant fractions is somewhat unexpected and encouraging for the use of this method in mineral wastes.

In contaminated soil remediation the low removal and mobilization of Pb has been highlighted in previous works [14, 33, 38-42] due to its high affinity for sorption onto soil particles and precipitation as the highly insoluble mineral anglesite ($PbSO_4$). This is reflected by the order of adsorption selectiveness reported by Reddy et al. [6] for different clay soils which sees the following trend: Pb > Cu > Zn > Ca > Cd > Mg. In the case of waste treatment, although the mineralogical composition is not comparable (partly only for the mine tailings) Pb seems to follow the same behaviour especially when compared to Zn. The higher mobility of Zn is likely to be related to the higher solubility of Sphalerite (ZnS) compared to Galena (PbS) which is far less reactive due to the formation of anglesite [43].

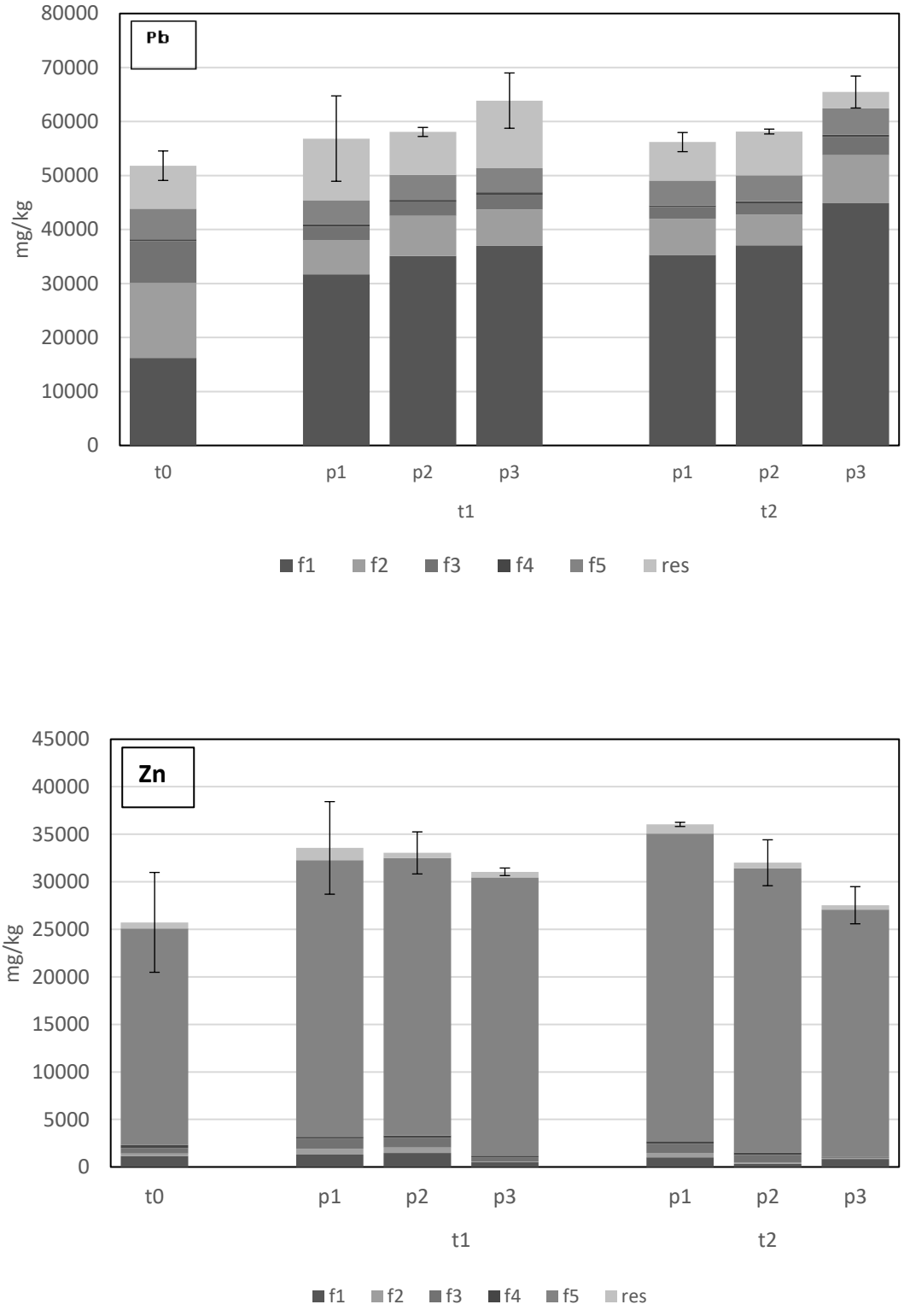

Figure 7. Total Pb and Zn distribution in MT with time and position (average values from duplicate specimens; error bars represent the range of the total metal recovery from all fractions).

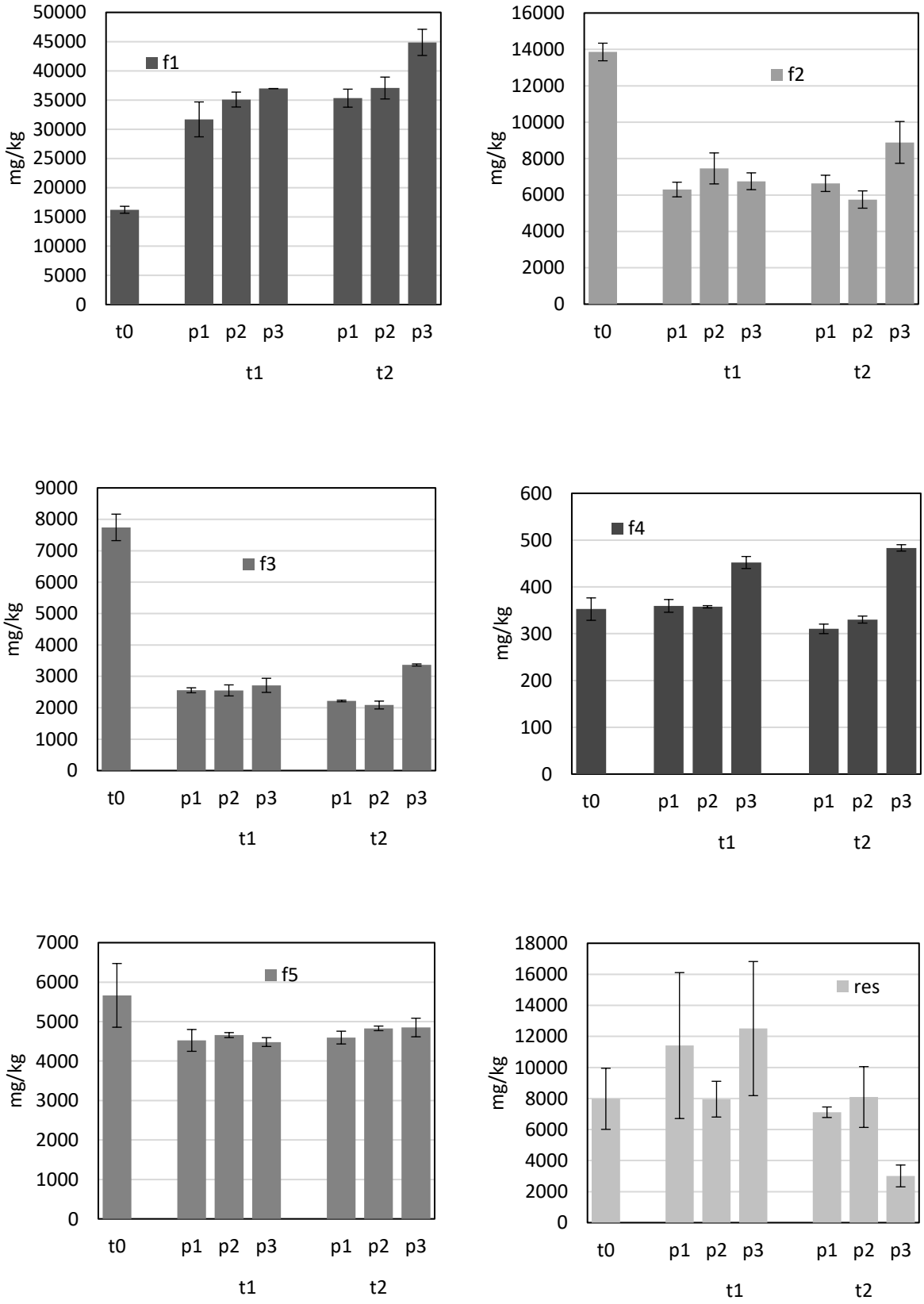

Figure 8. Pb distribution with time and position for individual fractions (MT) (average values from duplicate specimens; error bars represent the range of the recovery from the fraction).

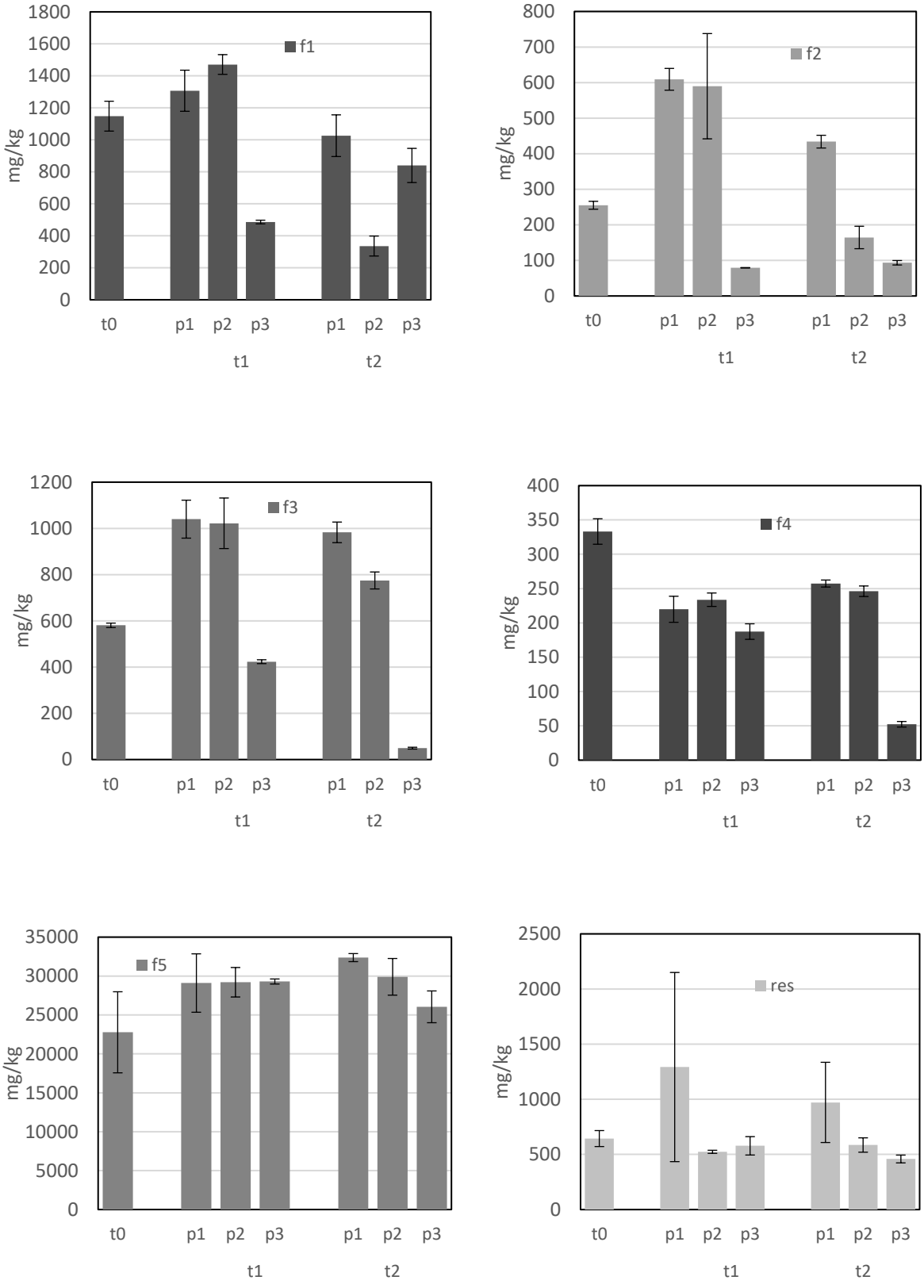

Figure 9. Zn distribution with time and position for individual fractions (MT) (average values from duplicate specimens; error bars represent the range of the recovery from the fraction).

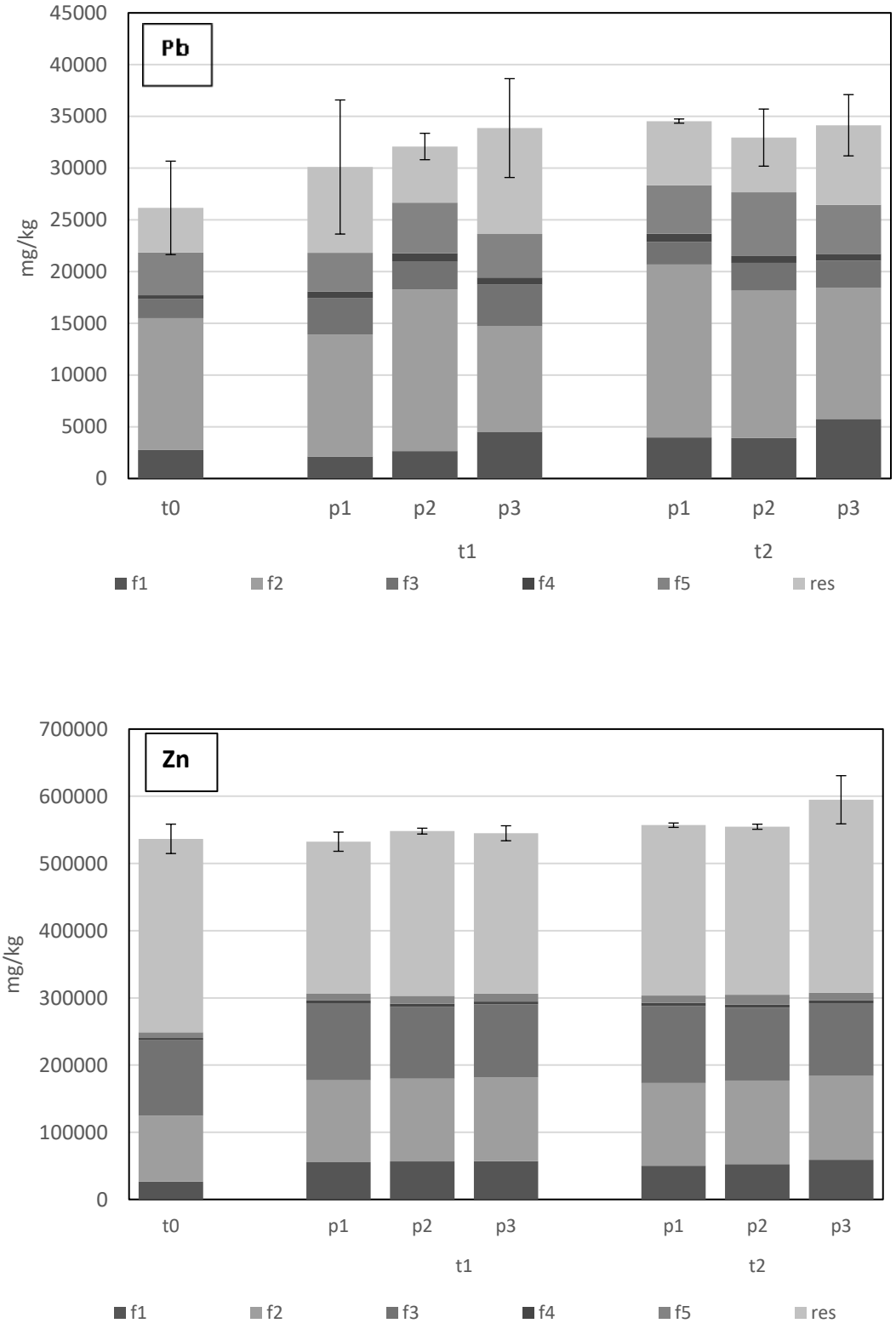

Figure 10. Total Pb and Zn distribution in EAFD with time and position (average values from duplicate specimens; error bars represent the range of the total metal recovery from all fractions).

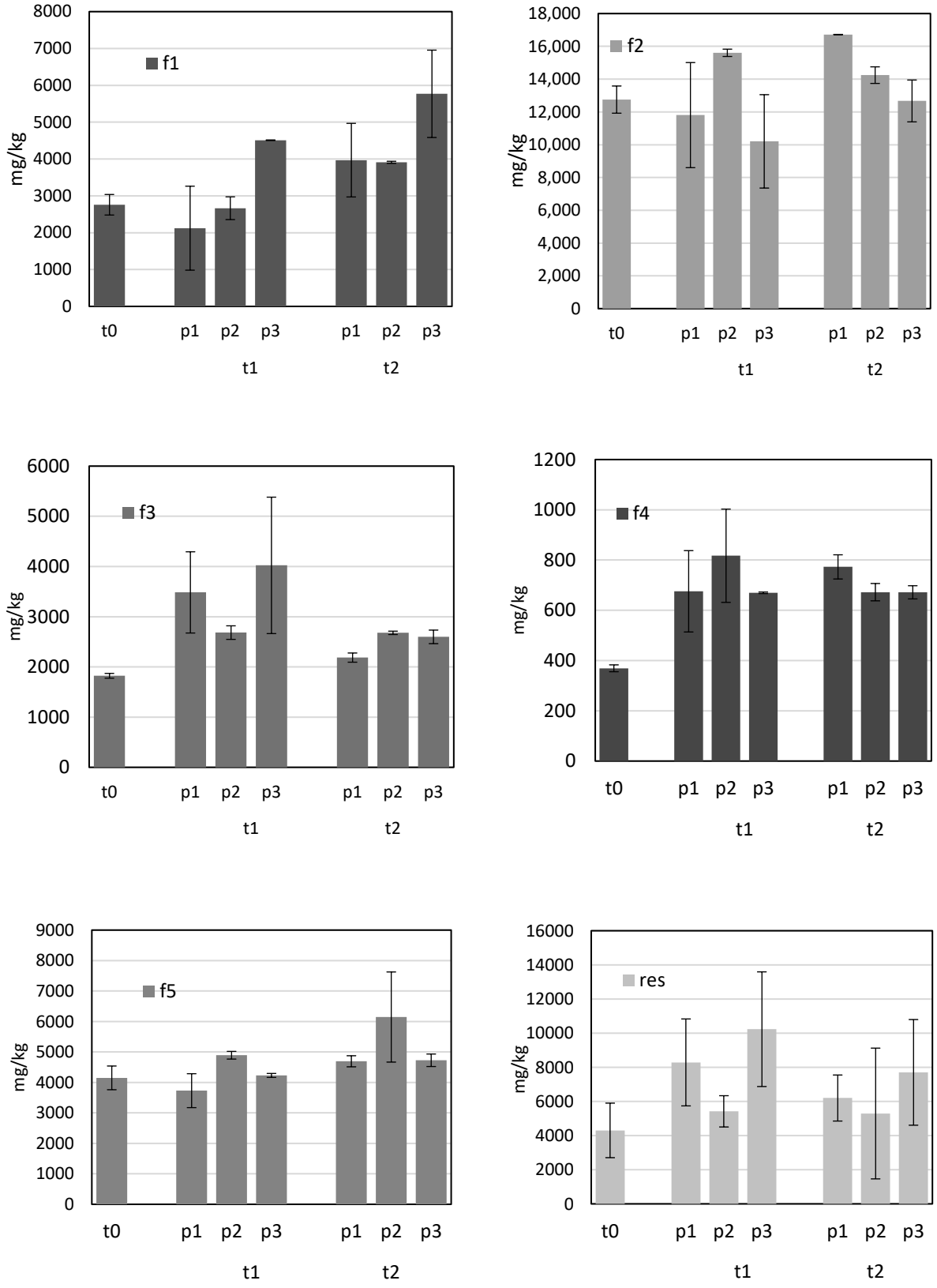

Figure 11. Pb distribution with time and position for individual fractions (EAFD) (average values from duplicate specimens; error bars represent the range of the recovery from the fraction).

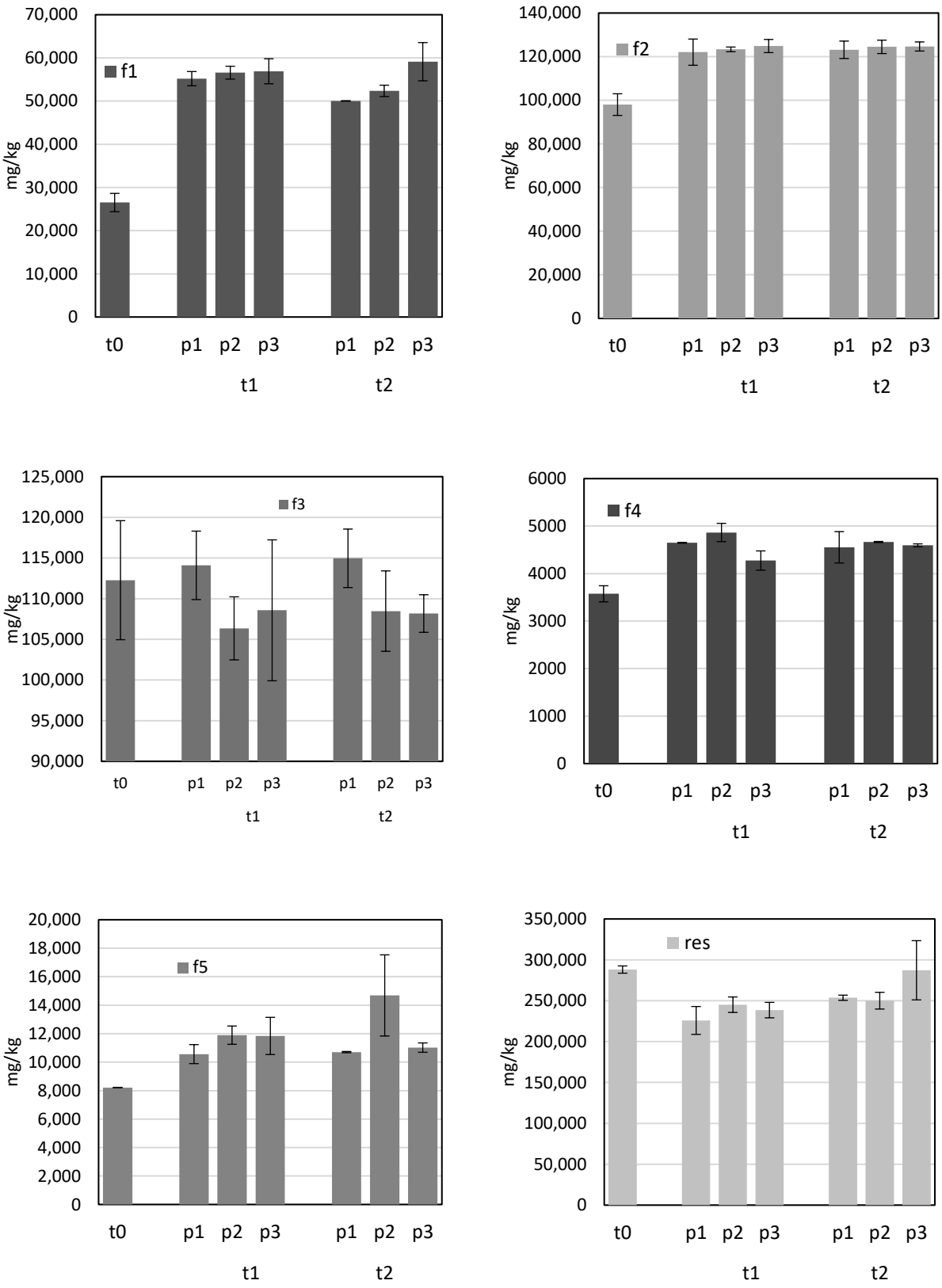

Figure 12. Zn distribution with time and position for individual fractions (EAFD) (average values from duplicate specimens; error bars represent the range of the recovery from the fraction).

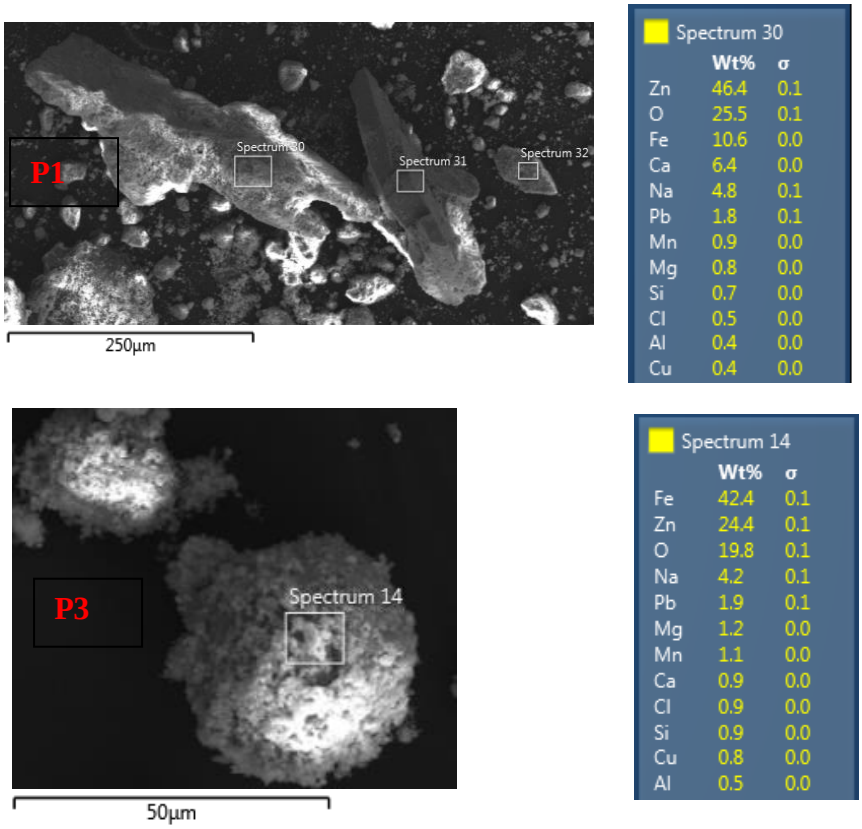

Figure 13. SEM images of the EAFD sample in P1 and P3 at time t2.

4. Conclusions

It is possible to make the following conclusions from the experimental data presented above:

- The two materials examined are characterised by two very different starting pH and buffering capacities, characteristics demonstrated to be particularly important for the effectiveness of the EK treatment for extracting Pb and Zn. The acidic front progressing and gradually lowering the pH from anode to cathode was more marked in the MT material due to its lower buffering capacity compared to EAFD where little pH change was observed.
- In MT ZnS and PbS were the mineral phases controlling the solubilisation of Pb and Zn. The likely source of the Zn solubilised by EK treatment of the EAFD is the ZnO and Zn-bearing Fe_2O_4. Whilst the source of Pb is not clearly highlighted. For the mine tailings the higher mobility of Zn relative to Pb is given by the higher solubility of ZnS compared to PbS which is far less reactive due to the formation of $PbSO_4$.
- In MT the SSE profiles at the end of EK suggest that the acid generation has significantly altered the distribution of the metals, while overall Pb is not removed but repartitioned towards the more available fractions; for Zn the fractions that are most affected by a change in pH, all show a gradual reduction at p3 and transport towards p1.

- The application of the electric field in EAFD showed much less effect compared to MT, likely to be due to the very high pH conditions. The interpretation of the SSE, supported by the SEM images, suggests that re-precipitation of metals in the f2 fraction as hydroxides or other minerals is taking place in the bulk of the material, together with the removal of Zn from the Fe-oxides phases in the region of lower pH and higher oxidation capacity.

The changes in pH and redox potential arising as a result of the application of an electric field are likely to be the main causes of the changes in speciation of both Zn and Pb observed here. The present conditions were demonstrated to be not sufficient to induce substantial metal removal from the wastes in the relatively short duration of these tests. However, the considerable changes in metal fractionation, including in fractions traditionally considered to be unavailable to EK, suggests that more intensive or longer-term processing, potentially coupled with use of leaching enhancement agents, could lead to significant mobilisation and extraction of valuable resource from wastes such as these.

Going beyond the removal of metals from the relatively available fractions represents a step forward from the application of EK in soil remediation since the metals present in such large repositories can be considered as not only contaminants, but as potentially valuable secondary resources. The economic disincentive to recovering metals from industrial wastes often relates to the low grade of target metals and/or recalcitrance of the host matrix such that the benefit of metals recovery is outweighed by the need for costly excavation and processing. It is therefore important to explore in situ techniques such as EK which, when applied judiciously to the right wastes can not only recover labile metals but as demonstrated here, may also affect changes to the fundamental structure of the waste to release the target metals for transport and extraction. EK has faced several limitations in the large scale applications involving excessive energy consumption and limited depth of penetration. However, the results presented in this study have shown that the technique can lead to the redistribution of metals from more recalcitrant phases to more labile fractions, thereby increasing the proportion of metals which can be extracted in situ, either by EK or chelant-enhanced EK, which may help to overcome resistance to use of the technique at full scale due to the issues highlighted above. When considering the unparalleled in situ applicability of EK to repositories of fine grained and heterogeneous wastes, it is clear that the technique has the capacity to offer considerable advantages over ex situ recovery methods, avoiding the costly excavation and processing that these methods entail. As such this work has the potential to lead towards the development of approaches that are able to turn waste materials into asset by transforming them into viable ore deposits.

References

1. USEPA, *In Situ Remediation Technology Statu Report: Electrokinetics*, in *US EPA Research Report*, S.W.a.E. Response, Editor. 1995, EPA.
2. Lageman, R., *Electroreclamation. Applications in the Netherlands.* Environmental Science & Technology, 1993. **27**(13): p. 2648-2650.
3. Acar, Y.B., et al., *Electrokinetic remediation: basics and technology status.* Journal of Hazardous Materials, 1995. **40**(2): p. 117-137.
4. Cauwenberghe, L.V., *Electrokinetics* Technology overview report TO-97-03, ed. C. Ground-water Remediation Technologies Analysis. 1997, Pittsburgh, PA: Ground-Water Remediation Technology Analysis Center.
5. Acar, Y.B. and A.N. Alshawabkeh, *Principles of electrokinetic remediation.* Environmental science & technology, 1993. **27**(13): p. 2638-2647.
6. Reddy, K.R. and C. Cameselle, *Electrochemical remediation technologies for polluted soils, sediments and groundwater*. 2009: John Wiley & Sons.
7. Crane, R.A., et al., *Physicochemical composition of wastes and co-located environmental designations at legacy mine sites in the south west of England and Wales: Implications for their resource potential.* Resources, Conservation and Recycling.
8. Sapsford, D., P. Cleall, and M. Harbottle, *In Situ Resource Recovery from Waste Repositories: Exploring the Potential for Mobilization and Capture of Metals from Anthropogenic Ores.* Journal of Sustainable Metallurgy, 2017. **3**(2): p. 375-392.
9. Zhu, N.-m., et al., *Electrokinetic removal of Cu and Zn in anaerobic digestate: Interrelation between metal speciation and electrokinetic treatments.* Journal of Hazardous Materials, 2015. **286**(0): p. 118-126.
10. Guiqun Peng, G.T., Junzhi Liu, Qibei Bao, Ling Zang, *Removal of heavy metals from sewage sludge with a combination of bioleaching and electrokinetic remediation technology*. Desalination, 2011.
11. Pedersen, A.J., L.M. Ottosen, and A. Villumsen, *Electrodialytic removal of heavy metals from different fly ashes: Influence of heavy metal speciation in the ashes.* Journal of Hazardous Materials, 2003. **100**(1–3): p. 65-78.
12. Rojo, A., et al., *Electrodialytic remediation of copper mine tailings: Comparing different operational conditions.* Minerals Engineering, 2006. **19**: p. 500-504.
13. Reddy, K.R., C.Y. Xu, and S. Chinthamreddy, *Assessment of electrokinetic removal of heavy metals from soils by sequential extraction analysis.* Journal of Hazardous Materials, 2001. **84**(2–3): p. 279-296.
14. Kim, S.-O. and K.-W. Kim, *Monitoring of electrokinetic removal of heavy metals in tailing-soils using sequential extraction analysis.* Journal of Hazardous Materials, 2001. **85**(3): p. 195-211.
15. Tessier, A., P.G.C. Campbell, and M. Bisson, *Sequential extraction procedure for the speciation of particulate trace metals.* Analytical Chemistry, 1979. **51**(7): p. 844-851.
16. FÖRSTNER, W.S.a.U., *Metals in the Hydrocycle. Berlin — Heidelberg — New York — Tokyo: Springer Verlag, 349 S., 149 Abb., DM 98.—*. Acta hydrochimica et hydrobiologica, 1985. **13**(2): p. 267-267.
17. Mester, Z., et al., *Comparison of two sequential extraction procedures for metal fractionation in sediment samples.* Analytica Chimica Acta, 1998. **359**(1): p. 133-142.

18. Dold, B., *Speciation of the most soluble phases in a sequential extraction procedure adapted for geochemical studies of copper sulfide mine waste.* Journal of Geochemical Exploration, 2003. **80**(1): p. 55-68.
19. Hansen, H.K., et al., *Speciation and mobility of cadmium in straw and wood combustion fly ash.* Chemosphere, 2001. **45**(1): p. 123-128.
20. Esakku, S., et al., *Assessment of heavy metal species in decomposed municipal solid waste.* Chemical Speciation & Bioavailability, 2005. **17**(3): p. 95-102.
21. BSI, *BS 1377-3:1990 Methods of test for soils for civil engineering purposes. Chemical and electro-chemical tests*. 1990.
22. BSI, *BS 1377-2:1990 Methods of test for soils for civil engineering purposes. Classification tests*. 1990.
23. Vane, L.M. and G.M. Zang, *Effect of aqueous phase properties on clay particle zeta potential and electro-osmotic permeability: Implications for electro-kinetic soil remediation processes.* Journal of Hazardous Materials, 1997. **55**(1–3): p. 1-22.
24. Yukselen, Y. and A. Kaya, *Zeta Potential of Kaolinite in the Presence of Alkali, Alkaline Earth and Hydrolyzable Metal Ions.* Water, Air, and Soil Pollution, 2003. **145**(1-4): p. 155-168.
25. Kaya, A. and Y. Yukselen, *Zeta potential of clay minerals and quartz contaminated by heavy metals.* Canadian Geotechnical Journal, 2005. **42**(5): p. 1280-1289.
26. BSI, *DD CEN/TS 15364:2006: "Characterization of waste. Leaching behaviour tests. Acid and base neutralization capacity test"*. 2006.
27. Yeung, A.T., *Milestone developments, myths, and future directions of electrokinetic remediation.* Separation and Purification Technology, 2011. **79**(2): p. 124-132.
28. Laforest, G. and J. Duchesne, *Characterization and leachability of electric arc furnace dust made from remelting of stainless steel.* Journal of Hazardous Materials, 2006. **135**(1–3): p. 156-164.
29. Stegemann, J.A., et al., *Understanding Environmental Leachability of Electric Arc Furnace Dust.* Journal of Environmental Engineering, 2000. **126**(2): p. 112-120.
30. Machado, J.G.M.S., et al., *Chemical, physical, structural and morphological characterization of the electric arc furnace dust.* Journal of Hazardous Materials, 2006. **136**(3): p. 953-960.
31. Kirkelund, G.M., L.M. Ottosen, and A. Villumsen, *Investigations of Cu, Pb and Zn partitioning by sequential extraction in harbour sediments after electrodialytic remediation.* Chemosphere, 2010. **79**(10): p. 997-1002.
32. Palumbo-Roe, B., et al., *Prediction of the long-term performance of abandoned lead zinc mine tailings in a Welsh catchment.* Journal of Geochemical Exploration, 2009. **100**(2–3): p. 169-181.
33. Kim, S.O., K.W. Kim, and D. Stuben, *Evaluation of electrokinetic removal of heavy metals from tailing soils.* Journal of Environmental Engineering-Asce, 2002. **128**(8): p. 705-715.
34. Song, Y., et al., *Effect of EDTA, EDDS, NTA and citric acid on electrokinetic remediation of As, Cd, Cr, Cu, Ni, Pb and Zn contaminated dredged marine sediment.* Environmental Science and Pollution Research, 2016. **23**(11): p. 10577-10586.
35. Fadlalla, H. and A.N. Alshawabkeh, *Efficacy of Electrolytic Generation and Transport of Oxygen for Soil Remediation*, in *5th ICEG Environmental Geotechnics: Opportunities, Challenges and Responsibilities for Environmental Geotechnics*. 2006. p. 126-132.
36. Lowson, R.T., *Aqueous oxidation of pyrite by molecular oxygen.* Chemical reviews, 1982. **82**(5): p. 461-497.

37. Gao, J., et al., *Effects of electrokinetic treatment of contaminated sludge on migration and transformation of Cd, Ni and Zn in various bonding states.* Chemosphere, 2013. **93**(11): p. 2869-2876.
38. Yang, J.-S., et al., *The transport behavior of As, Cu, Pb, and Zn during electrokinetic remediation of a contaminated soil using electrolyte conditioning.* Chemosphere, 2014. **117**(0): p. 79-86.
39. Kim, S.-O., S.-H. Moon, and K.-W. Kim, *Removal of Heavy Metals from Soils using Enhanced Electrokinetic Soil Processing.* Water, Air, and Soil Pollution, 2001. **125**(1): p. 259-272.
40. Pedersen, A.J., L.M. Ottosen, and A. Villumsen, *Electrodialytic removal of heavy metals from municipal solid waste incineration fly ash using ammonium citrate as assisting agent.* Journal of hazardous materials, 2005. **122**(1-2): p. 103-109.
41. Merkx, O.K., et al., *The Effectiveness of Electro-Remediation of Aged, Metal-Contaminated Sediment in Relation to Sequential Extraction of Metals.* Water, Air and Soil Pollution, 2013. **224**(9): p. 1-12.
42. Ottosen, L.M., K. Lepkova, and M. Kubal, *Comparison of electrodialytic removal of Cu from spiked kaolinite, spiked soil and industrially polluted soil.* Journal of Hazardous Materials, 2006. **137**(1): p. 113-120.
43. Hudson-Edwards, K.A., H.E. Jamieson, and B.G. Lottermoser, *Mine wastes: past, present, future.* Elements, 2011. **7**(6): p. 375-380.